



LAWRENCE  
LIVERMORE  
NATIONAL  
LABORATORY

# Progress in detailed modelling of low foot and high foot implosion experiments on the National Ignition Facility

D. S. Clark

November 25, 2015

9th International Conference on Inertial Fusion Science and Applications  
Bellevue, WA, United States  
September 20, 2015 through September 25, 2015

## **Disclaimer**

---

This document was prepared as an account of work sponsored by an agency of the United States government. Neither the United States government nor Lawrence Livermore National Security, LLC, nor any of their employees makes any warranty, expressed or implied, or assumes any legal liability or responsibility for the accuracy, completeness, or usefulness of any information, apparatus, product, or process disclosed, or represents that its use would not infringe privately owned rights. Reference herein to any specific commercial product, process, or service by trade name, trademark, manufacturer, or otherwise does not necessarily constitute or imply its endorsement, recommendation, or favoring by the United States government or Lawrence Livermore National Security, LLC. The views and opinions of authors expressed herein do not necessarily state or reflect those of the United States government or Lawrence Livermore National Security, LLC, and shall not be used for advertising or product endorsement purposes.

# Progress in detailed modelling of low foot and high foot implosion experiments on the National Ignition Facility

D. S. Clark, M. M. Marinak, C. R. Weber, D. C. Eder, S. W. Haan, B. A. Hammel, D. E. Hinkel, O. S. Jones, A. L. Kritcher, J. L. Milovich, P. K. Patel, H. F. Robey, J. D. Salmonson, and S. M. Sepke

Lawrence Livermore National Laboratory, Livermore, CA, USA

clark90@llnl.gov

**Abstract.** Several dozen high convergence inertial confinement fusion ignition experiments have now been completed on the National Ignition Facility (NIF). These include both “low foot” experiments from the National Ignition Campaign (NIC) and more recent “high foot” experiments. At the time of the NIC, there were large discrepancies between simulated implosion performance and experimental data. In particular, simulations over predicted neutron yields by up to an order of magnitude, and some experiments showed clear evidence of mixing of ablator material deep into the hot spot that could not be explained at the time. While the agreement between data and simulation improved for high foot implosion experiments, discrepancies nevertheless remain. This paper describes the state of detailed modelling of both low foot and high foot implosions using 1-D, 2-D, and 3-D radiation hydrodynamics simulations with HYDRA. The simulations include a range of effects, in particular, the impact of the plastic membrane used to support the capsule in the hohlraum, as well as low-mode radiation asymmetries tuned to match radiography measurements. The same simulation methodology is applied to low foot NIC implosion experiments and high foot implosions, and shows a qualitatively similar level of agreement for both types of implosions. While comparison with the experimental data remains imperfect, a reasonable level of agreement is emerging and shows a growing understanding of the high-convergence implosions being performed on NIF.

## 1. Introduction

Substantial progress has been made in modeling and understanding of ignition implosions on the National Ignition Facility (NIF) since the 2013 IFSA Conference. Since that time, hydrodynamic instability growth spectra have been measured for a range of perturbation mode numbers and for high foot as well as low foot implosion types [1]. These measurements have so far largely validated the simulation technique used to model NIF implosions, although measurements at higher convergence [2] and with better resolution are needed. In addition, the high foot implosion platform has been pushed to higher implosion velocities using higher laser powers and energies, and also thinner ablaters, and appear to show evidence of a ceiling in high foot performance. From the simulation perspective, detailed 3-D capsule-only simulations are showing increasing levels of agreement with NIF implosion measurements. Of equal importance, these detailed simulations have now been compared for representative low foot [3] and high foot [4] implosion types, and show similar levels of agreement with the data for these quite different implosion types. This paper summarizes recent progress in 3-D

simulations of NIF implosions using the radiation hydrodynamics code HYDRA [5]. The different implosion characteristics, as revealed in simulations of low as compared to high foot implosions, and their different failure modes are particularly important as these indicate where each implosion type may be improved and how a route to ignition on NIF may finally be achieved.

## 2. 3-D simulation results

3-D capsule-only simulations were run following the methodology described in Ref. [6]. Since the simulations in Ref. [6] were completed, however, further 2-D simulation work suggested that the perturbation seeded by the capsule support tent was even larger than assumed in those simulations. The understanding of the low-mode radiation flux asymmetries imprinted on the capsule from the hohlraum has also improved. For these reasons, the NIF implosion simulated in Ref. [6] (N120321, the highest compression implosion yet fired on NIF) was rerun with these updated inputs. Two additional implosion experiments have also been simulated: N120405 (a higher power and energy companion to N120321 that “mixed” heavily with  $\sim 1 \mu\text{g}$  of ablator material believed to have entered the hot spot) and N130927 (a high power foot implosion that showed the first evidence of “fuel gain,” that is, a fusion neutron yield equal to or greater than the peak fuel kinetic energy). It is important to understand the behavior of N120405 as it clearly crossed a performance “cliff” compared to N120321, and understanding the origin of this cliff—the source of the hot spot mix mass in particular—is essential in avoiding this fate in future implosions. It is equally important to contrast the results of the low foot implosions (N120321 and N120405) against the high foot to understand the different strengths, and weaknesses, of these quite different implosion types.

Figure 1 contrasts the results from 3-D simulations of each of these shots at their respective bang times (time of peak neutron production). In each case, the outer surface is the ablation front colored by the electron temperature, the left cutaway shows the ion temperature, and the right cutaway shows

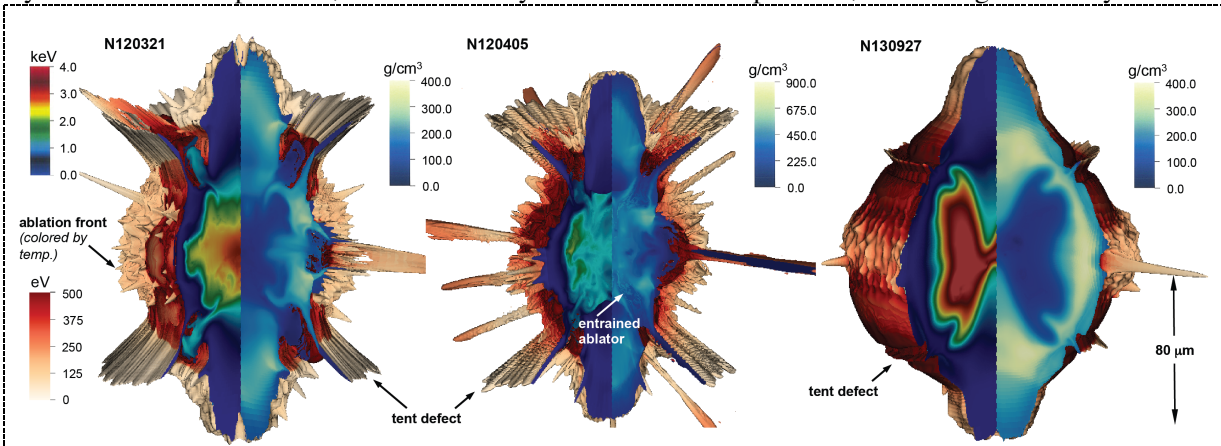
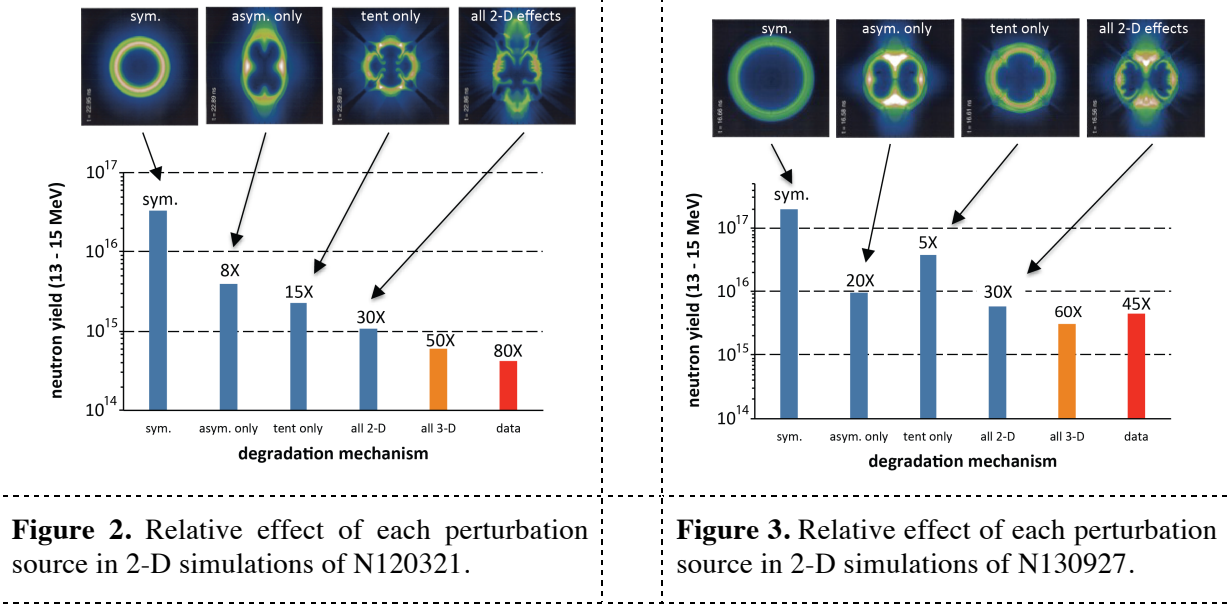


**Figure 1.** Comparison of 3-D simulation results for N120321, N120405, and N130927 at their respective bang times. Temperature color scales are the same between all three simulations but the density scales differ.

the density. The large “sombrero hat” features in both of the low foot implosions result from ablation front instability growth seeded by the capsule support tent. As is clear from the figure, the tent is the dominant perturbation in these low foot implosions. In fact, in the case of N120405, it can be seen that the tent perturbation has grown so extreme that it has entrained plastic ablator material into the center of the hot spot. This appears to explain the source of the hot spot mix mass observed for this shot: the stronger acceleration and hence ablation front instability growth of N120405 amplified the tent perturbation to such an extent that the already large perturbation on N120321 grew so large as to enter the hot spot on N120405. Note that the tent perturbation encircles the full azimuth of the capsule at each pole and hence gives a large area for ablator material to suddenly enter the hot spot once an amplitude threshold is passed. In contrast, the high foot implosion N130927 is clearly much less

perturbed at the ablation front. While a small tent defect is evident in this simulation, it is much reduced relative to the low foot, and the dominant perturbation source is now the hohlraum radiation asymmetry. This asymmetry results in the large spikes or jets entering the north and south poles of the hot spot in this simulation. Even so, a much larger and hotter hot spot results compared to the low foot, and hence this implosion gives a much higher yield.

To quantify the relative importance of the various perturbation sources in the low foot and high foot implosion types, Figures 2 and 3 show the results of 2-D simulations run with each perturbation source included separately, namely, the hohlraum flux asymmetries alone, the tent perturbation alone,



all 2-D effects in combination, and finally the 3-D result from the simulations described above. The histogram shows the impact on the neutron yield with each effect, and the insets show the 2-D simulation results at bang time. For the low foot implosion N120321, the tent is quantitatively the largest impact resulting in a 15 $\times$  yield degradation relative to 1-D. This is nearly twice the impact of the flux asymmetries that result in an 8 $\times$  degradation. As shown in Figure 2, these roles reverse for the high foot. The better ablation front stability of the high foot reduces the impact of the tent to a 5 $\times$  reduction in yield relative to 1-D, while the hohlraum asymmetries result in a 20 $\times$  degradation. Interestingly, for the high foot, the 2-D simulation with all effects included is fairly close to the measured yield data and the 3-D simulation actually under-predicts the yield. By contrast, for the low foot, the 2-D simulation including all effects over-predicts the yield by more than a factor of two, while only the 3-D simulation is fairly close to the measured yield. This is indicative of the generally larger perturbation levels in low foot implosions that can only be accurately captured in a fully 3-D simulation.

Quantitative comparisons of the 3-D simulation results against the data for the three shots simulated are summarized in Table 1. The rows list a number of the principle experimental observables and pairs of columns compare the simulation results against the data for each successive shot. The agreement is generally good for all three shots, although many quantities are not matched within the experimental error bars. In these cases, the simulation results are generally within two error bars of the data, however. In comparing the primary neutron image size (PNI  $P_0$ ), down scattered neutron image size (DSNI  $P_0$ ), burn-averaged ion temperature ( $T_{ion}$ ), and neutron down scattered ratio (DSR), an important caveat should be pointed out. Given the scale of these 3-D simulations, current computing capabilities do not allow running the simulations with inline Monte Carlo neutronics, as is routinely done in 2-D. The simulation values listed in the table are hence taken from instantaneous post-processing of the simulations at bang time. As such, they represent snapshots of the state of the simulation at bang time and omit the time averaging over the duration of the burn that is inherent in

the measurement and would be included if these quantities could be computed inline. This limitation in the current simulations may account for the noticeable discrepancies in the simulated DSR for N120321 and also in the ion temperatures for N120321 and N130927. It is, of course, possible that these discrepancies point to inadequacies in the physical models used in the simulations or are the result of imperfect knowledge of the initial and boundary conditions for these shots. At this time, it is not possible to resolve which of these possibilities is responsible. Nevertheless, the overall agreement between the simulations and the data is quite good. This is notable given that three quite different shots have been simulated, and each appears to agree equally well with the experimental results.

**Table 1.** Comparison of simulation and experimental results for N120321, N120405, and N130927.

	N120321		N120405		N130927	
	sim.	expt.	sim.	expt.	sim.	expt.
bang time (ns)	22.85	22.91±0.04	22.53	22.70±0.08	16.53	16.59±0.03
burn width (ps)	167	158±40	130	161±40	143.5	188±30
x-ray $P_0$ (μm)	21.9	20.1±1.4	23.9	23.4±0.85	31.4	35.3±3.0
x-ray $M_0$ (μm)	19.8	22.7±2.7	24.1	26.5±4.0	45.7	49.8±1.5
PNI $P_0$ (μm)	24.4	26±3	25.4	27±3	27.7	32±4
DSNI $P_0$ (μm)	38.4	35±3	31.7	43±6	51.1	55±4
$T_{\text{ion}}$ (keV)	2.6	3.1±0.4	1.7	1.69±0.13	3.9	4.43±0.15
DSR (%)	5.0	6.2±0.6	5.5	5.14±0.29	3.5	3.48±0.17
$Y_{13-15 \text{ MeV}}$	$6.0 \times 10^{14}$	$4.2 \pm 0.1 \times 10^{14}$	$1.4 \times 10^{14}$	$1.3 \pm 0.1 \times 10^{14}$	$3.1 \times 10^{15}$	$4.5 \pm 0.1 \times 10^{15}$

### 3. Conclusions

Three ignition implosion experiments from the NIF database have been simulated following the most up-to-date 3-D simulation methodology. All three show reasonably good, though not perfect, agreement with the experimental data. Given that these three shots explored quite different regions of implosion parameter space, the agreement suggests that a fairly robust simulation capability is developing for accurately modeling the high convergence implosions being tested on NIF. This validated simulation capability is clearly essential for assessing what design modifications can lead to further gains in implosion performance.

### Acknowledgements

This work was performed under the auspices of the U.S. Department of Energy by Lawrence Livermore National Laboratory under Contract DE-AC52-07NA27344.

### References

- [1] Smalyuk V A, *et al.* 2014 *Phys. Plasmas* **21** 056301
- [2] Hammel B A, *et al.* 2015, *Bull. Am. Phys. Soc.* **60** 164
- [3] Edwards M J, *et al.* 2013 *Phys. Plasmas* **20** 070501
- [4] Hurricane O A, *et al.* 2014 *Phys. Plasmas* **21** 056314
- [5] Marinak M M, *et al.* 2001 *Phys. Plasmas* **8** 2275
- [6] Clark D S, *et al.* 2015 *Phys. Plasmas* **22** 022703